

Exact stationary solutions of the Kolmogorov-Feller equation in a bounded domain

S.I. Denisov*, Yu.S. Bystrik

Sumy State University, 2 Rimsky-Korsakov Street, UA-40007 Sumy, Ukraine

Abstract

We present the first detailed analysis of the statistical properties of jump processes bounded by a saturation function and driven by Poisson white noise, being a random sequence of delta pulses. The Kolmogorov-Feller equation for the probability density function (PDF) of such processes is derived and its stationary solutions are found analytically in the case of the symmetric uniform distribution of pulse sizes. Surprisingly, these solutions can exhibit very complex behavior arising from both the boundedness of pulses and processes. We show that all features of the stationary PDF (number of branches, their form, extreme values probability, etc.) are completely determined by the ratio of the saturation function width to the half-width of the pulse-size distribution. We verify all theoretical results by direct numerical simulations.

Keywords: Bounded processes, Poisson white noise, Kolmogorov-Feller equation, Exact stationary solutions

1. Introduction

The Langevin equation (i.e., a stochastic ordinary differential equation) is widely used for studying stochastic systems in physics, chemistry, engineering and other areas [1]. In the simplest case when the random force noise is Gaussian and white the dynamics of the system is Markovian and its probability density function (PDF) satisfies the Fokker-Planck equation [2, 3, 4]. One of the advantages of this approach is that the Fokker-Planck equation can often be solved analytically, especially in the stationary regime.

*Corresponding author

Email address: `denisov@sumdu.edu.ua` (S.I. Denisov)

If Gaussian noise is colored, then the system dynamics becomes non-
10 Markovian and the corresponding PDF obeys the integro-differential master
equation, which under certain conditions can be reduced to the differential
one by the Kramers-Moyal expansion [1, 2]. Since, in general, this differential
equation is of infinite order, several approximation schemes for its simplifica-
tion were proposed [5, 6, 7] (for a recent theoretical and numerical analysis
15 see, e.g., Refs. [8, 9] and references therein). Note also that in some very
special cases when the Langevin equation is solved analytically the PDFs
can be determined straightforwardly [3, 10, 11, 12].

The Langevin equation driven by Poisson white noise (sometimes called a
train of delta pulses), which is a particular case of non-Gaussian white noises,
20 plays an important role in describing the jump processes and phenomena
induced by this noise in different systems (see, e.g., Refs. [13, 14, 15, 16,
17]). More recent studies include noise-induced transport [18, 19], stochastic
resonance [20], vibro-impact response [21, 22] and ecosystem dynamics [23,
24], to name only a few. The determination of the corresponding PDF is
25 a much more difficult problem than for Gaussian white noise, because the
master equation is integro-differential. Note in this connection that even for
the first-order Langevin equation the master equation reduces to the integro-
differential Kolmogorov-Feller equation, whose exact stationary solutions are
known only in a few cases [25, 26, 27, 28, 29].

30 Often the bounded processes more adequately describe the stochastic be-
havior of real systems than the unbounded ones [30]. But the bounded jump
processes driven by Poisson white noise, which could be used, for example,
to model the destruction phenomena, have not been studied in depth. As far
as we know, our recent paper [31] is the only one devoted to the analytical
35 study of the statistical properties of such processes. It has been shown, in
particular, that the jump character and boundedness of these processes are
responsible for the nonzero probability of their extremal values and nonuni-
formity of their distribution inside a bounded domain.

In this work, we generalize the difference Langevin equation describing
40 bounded jump processes driven by Poisson white noise, derive the corre-
sponding Kolmogorov-Feller equation and solve it analytically in the sta-
tionary state for the case of uniform distribution of pulse sizes. The paper is
organized as follows. In Section 2, using the saturation function, we introduce
the difference Langevin equation driven by Poisson white noise, whose solu-
45 tions are bounded. The Kolmogorov-Feller equation that corresponds to this
Langevin equation is derived in Section 3. In the same section, we cast the

stationary solution of the Kolmogorov-Feller equation as a sum of singular terms defining the probability of the extremal values of the bounded process and a regular part representing the non-normalized PDF of this process inside a bounded domain. In [Section 4](#), which is the main section of the paper, we solve analytically the integral equation for the non-normalized PDF and calculate the extreme values probability in the case of uniform distribution of pulse sizes. Here, we show that the ratio of the saturation function width to the half-width of the pulse-size distribution is the only parameter that determines all features of the non-normalized PDF, including its explicit form and complexity. Finally, our main findings are summarized in [Section 5](#).

2. Model for bounded stochastic processes

A variety of continuous-time processes in physics, biology, economics and other areas can be described by the first-order Langevin equation

$$\frac{d}{dt}X_t = F(X_t) + \xi(t), \quad (1)$$

which, for convenience, is often written in difference form

$$X_{t+\tau} = X_t + F(X_t)\tau + \Delta_\tau. \quad (2)$$

Here, X_t ($t \geq 0$) is a random process, $F(x)$ is a given deterministic function, $\xi(t)$ is a stationary white noise, τ is an infinitesimal time interval, and Δ_τ is a random variable defined as

$$\Delta_\tau = \int_t^{t+\tau} \xi(t') dt' = \int_0^\tau \xi(t') dt'. \quad (3)$$

The realizations of X_t can be either continuous (as in the case of Gaussian white noise) or discontinuous (as in the cases, e.g., of Lévy and Poisson white noises). These realizations are, in general, unbounded, i.e., the probability that $|X_t|$ exceeds a given level is nonzero. In order to extend the Langevin approach to the description of random processes in bounded domains, we introduce instead of [Eq. \(2\)](#) a more general difference Langevin equation

$$X_{t+\tau} = S(X_t + F(X_t)\tau + \Delta_\tau), \quad (4)$$

where

$$S(x) = \begin{cases} x, & |x| \leq l, \\ \text{sgn}(x)l, & |x| > l \end{cases} \quad (5)$$

is the saturation function, $2l$ is its width (domain size), and $\text{sgn}(x)$ is the signum function. According to Eq. (4) and definition (5), a nonlinear random process X_t is bounded, i.e., if $X_0 \in [-l, l]$, then X_t evolves in such a way that $|X_t| \leq l$ for all $t \geq 0$. Note, this equation reduces to Eq. (2) when $l \rightarrow \infty$.

Although in Eq. (4) any noise can be used, next we explore Poisson white noise only, which is defined as a sequence of delta pulses (see, e.g., Ref. [16] and references therein):

$$\xi(t) = \sum_{i=1}^{n(t)} z_i \delta(t - t_i). \quad (6)$$

Here, $n(t)$ denotes the Poisson counting process, which is characterized by the probability $Q_n(t) = (\lambda t)^n e^{-\lambda t} / n!$ that $n \geq 0$ events occur at random times t_i within a given time interval $(0, t]$, λ is the rate parameter, $\delta(\cdot)$ is the Dirac δ function, and z_i are independent random variables distributed with the same probability density $q(z)$ [$z \in (-\infty, \infty)$]. It is also assumed that this probability density is symmetric, $q(-z) = q(z)$, and $\xi(t) = 0$ if $n(t) = 0$. From (3) and (6) it follows that in the case of Poisson white noise the random variable Δ_τ is the compound Poisson process [16], i.e.,

$$\Delta_\tau = \begin{cases} 0, & n(\tau) = 0, \\ \sum_{i=1}^{n(\tau)} z_i, & n(\tau) \geq 1. \end{cases} \quad (7)$$

Since $\tau \rightarrow 0$, the probability density $p_\tau(z)$ that $\Delta_\tau = z$ is written in the linear approximation in τ as [27]

$$p_\tau(z) = (1 - \lambda\tau)\delta(z) + \lambda\tau q(z). \quad (8)$$

3. Kolmogorov-Feller equation

3.1. Time-depended case

Our next aim is to derive the Kolmogorov-Feller equation for the normalized time-depended PDF $P_t(x)$ of the bounded process X_t governed by Eq. (4). Using the definition $P_t(x) = \langle \delta(x - X_t) \rangle$, where $x \in [-l, l]$, the angular brackets denote averaging over all realizations of X_t , and two-step averaging procedure for $\langle \delta(x - X_{t+\tau}) \rangle$ [32], we can write

$$\begin{aligned} P_{t+\tau}(x) &= \langle \delta[x - S(X_t + F(X_t)\tau + \Delta_\tau)] \rangle \\ &= \int_{-l}^l P_t(x') \left(\int_{-\infty}^{\infty} p_\tau(z) \delta[x - S(x' + F(x')\tau + z)] dz \right) dx'. \end{aligned} \quad (9)$$

Taking also into account the representation

$$P_t(x) = \int_{-l}^l P_t(x') \left(\int_{-\infty}^{\infty} p_\tau(z) \delta(x - x') dz \right) dx' \quad (10)$$

(it holds due to the normalization condition $\int_{-\infty}^{\infty} p_\tau(z) dz = 1$ and shifting property of the δ function) and the definition $(\partial/\partial t)P_t(x) = \lim_{\tau \rightarrow 0} [P_{t+\tau}(x) - P_t(x)]/\tau$, from (9) and (10) one obtains

$$\frac{\partial}{\partial t} P_t(x) = \int_{-l}^l K(x, x') P_t(x') dx', \quad (11)$$

where

$$K(x, x') = \lim_{\tau \rightarrow 0} \frac{1}{\tau} \int_{-\infty}^{\infty} p_\tau(z) \{ \delta[x - S(x' + F(x')\tau + z)] - \delta(x - x') \} dz \quad (12)$$

($x, x' \in [-l, l]$) is the kernel of the master equation (11).

In order to derive the Kolmogorov-Feller equation associated with Eq. (4) at $\tau \rightarrow 0$, we first substitute the probability density (8) into (12). After integration over z one gets

$$K(x, x') = \lim_{\tau \rightarrow 0} \frac{1}{\tau} \left\{ (1 - \lambda\tau) \delta[x - S(x' + F(x')\tau)] - \delta(x - x') + \lambda\tau \int_{-\infty}^{\infty} q(z) \delta[x - S(x' + F(x')\tau + z)] dz \right\}. \quad (13)$$

Then, replacing $S(x' + F(x')\tau + z)$ by $S(x' + z)$ (this is possible because only terms of the order of τ in braces contribute to the limit) and taking into account that $S(x') = x'$ and, in the linear approximation,

$$\delta[x - S(x' + F(x')\tau)] = \delta(x - x') - \tau \frac{\partial}{\partial x} \delta(x - x') F(x'), \quad (14)$$

the kernel (13) can be rewritten in the form

$$K(x, x') = -\frac{\partial}{\partial x} \delta(x - x') F(x') - \lambda \delta(x - x') + \lambda \int_{-\infty}^{\infty} q(z) \delta[x - S(x' + z)] dz. \quad (15)$$

Finally, using in (15) the representation

$$\begin{aligned} \int_{-\infty}^{\infty} q(z)\delta[x - S(x' + z)] dz &= \delta(x + l) \int_{-\infty}^{-l-x'} q(z)dz + \delta(x - l) \int_{l-x'}^{\infty} q(z) dz \\ &+ \int_{-l-x'}^{l-x'} q(z)\delta(x - x' - z) dz, \end{aligned} \quad (16)$$

which directly follows from the definition (5) of the saturation function, the integral formula $\int_{-l-x'}^{l-x'} q(z)\delta(x - x' - z) dz = q(x - x')$, and the exceedance probability defined as

$$R(z) = \int_z^{\infty} q(z') dz' \quad (17)$$

[$R(-\infty) = 1$, $R(0) = 1/2$, $R(\infty) = 0$], we obtain

$$\begin{aligned} K(x, x') &= -\frac{\partial}{\partial x} \delta(x - x')F(x') - \lambda\delta(x - x') + \lambda\delta(x - l)R(l - x') \\ &+ \lambda\delta(x + l)R(l + x') + \lambda q(x - x'). \end{aligned} \quad (18)$$

Now, substituting this kernel into Eq. (11), we get the Kolmogorov-Feller equation

$$\begin{aligned} \frac{1}{\lambda} \frac{\partial}{\partial t} P_t(x) + \frac{1}{\lambda} \frac{\partial}{\partial x} F(x)P_t(x) + P_t(x) &= \delta(x - l) \int_{-l}^l R(l - x')P_t(x') dx' \\ &+ \delta(x + l) \int_{-l}^l R(l + x')P_t(x') dx' + \int_{-l}^l q(x - x')P_t(x') dx', \end{aligned} \quad (19)$$

65 which corresponds to the difference Langevin equation (4) with $\tau \rightarrow 0$
 (note, the Kolmogorov-Feller equation for $F(x) = 0$ has been derived in
 Ref. [31]). As usual, Eq. (19) should be supplemented by the normalization,
 $\int_{-l}^l P_t(x) dx = 1$, and initial, $P_0(x) = \delta(x - X_0)$, conditions. It should also
 be emphasized that, according to [31], any boundary conditions at $x = \pm l$
 70 are not needed to solve this equation.

3.2. Stationary PDF and its representation

Our future efforts will be focused only on the stationary PDF $P_{st}(x) = \lim_{t \rightarrow \infty} P_t(x)$ at $F(x) = 0$. Since by assumption $q(-z) = q(z)$, in this case

the stationary PDF is symmetric, $P_{\text{st}}(-x) = P_{\text{st}}(x)$, and, as it follows from Eq. (19), satisfies the integral equation

$$P_{\text{st}}(x) = [\delta(x-l) + \delta(x+l)] \int_{-l}^l R(l-x') P_{\text{st}}(x') dx' + \int_{-l}^l q(x-x') P_{\text{st}}(x') dx'. \quad (20)$$

According to [31], the general solution of Eq. (20) can be represented in the form

$$P_{\text{st}}(x) = a[\delta(x-l) + \delta(x+l)] + f(x), \quad (21)$$

where a is the probability that X_t in the stationary state equals l (or $-l$), and the non-normalized probability density $f(x)$ is symmetric, $f(-x) = f(x)$, and is governed by the integral equation

$$f(x) = a[q(x-l) + q(x+l)] + \int_{-l}^l q(x-x') f(x') dx'. \quad (22)$$

Using (21) and the normalization condition $\int_{-l}^l P_{\text{st}}(x) dx = 1$, the probability a of the extremal values of the process X_t in the stationary state can be expressed through the non-normalized PDF $f(x)$ as follows:

$$a = \frac{1}{2} - \int_0^l f(x) dx. \quad (23)$$

4. Exact solutions for uniform jumps

4.1. Basic equations

In order to solve Eq. (22) analytically, we restrict ourselves to the case when the jump magnitudes z_i are uniformly distributed on the interval $[-c, c]$ ($c > 0$ is the half-width of this distribution). In other words, we assume that the probability density $q(z)$ is given by

$$q(z) = \begin{cases} 1/2c, & |z| \leq c, \\ 0, & |z| > c. \end{cases} \quad (24)$$

Depending on the value of c , Eq. (22) can be rewritten in three different forms. First, if $c > 2l$, then

$$q(x-l) = q(x+l) = q(x-x') = \frac{1}{2c} \quad (25)$$

for all $x, x' \in [-l, l]$, and Eq. (22) reduces to

$$f(x) = \frac{a}{c} + \frac{1}{c} \int_0^l f(x') dx'. \quad (26)$$

Second, if $c \in (l, 2l)$, then

$$q(x-l) = \begin{cases} 0, & x \in [-l, l-c), \\ 1/2c, & x \in [l-c, l], \end{cases} \quad q(x+l) = \begin{cases} 1/2c, & x \in [-l, c-l], \\ 0, & x \in (c-l, l] \end{cases} \quad (27)$$

and

$$\int_{-l}^l q(x-x')f(x') dx' = \frac{1}{2c} \times \begin{cases} \int_{-l}^{x+c} f(x') dx', & x \in [-l, l-c], \\ \int_{-l}^l f(x') dx', & x \in [l-c, c-l], \\ \int_{x-c}^l f(x') dx', & x \in [c-l, l]. \end{cases} \quad (28)$$

Using these results, from Eq. (22) one obtains the following integral equations:

$$f(x) = \frac{a}{2c} + \frac{1}{2c} \int_{-l}^{x+c} f(x') dx' \quad (29a)$$

for $x \in [-l, l-c)$,

$$f(x) = \frac{a}{c} + \frac{1}{2c} \int_{-l}^l f(x') dx' \quad (29b)$$

for $x \in (l-c, c-l)$, and

$$f(x) = \frac{a}{2c} + \frac{1}{2c} \int_{x-c}^l f(x') dx' \quad (29c)$$

for $x \in (c-l, l]$.

And third, if $c \in (0, l)$, then the probability densities $q(x-l)$ and $q(x+l)$ are given by the same formulas (27), and

$$\int_{-l}^l q(x-x')f(x') dx' = \frac{1}{2c} \times \begin{cases} \int_{-l}^{x+c} f(x') dx', & x \in [-l, c-l], \\ \int_{x-c}^{x+c} f(x') dx', & x \in [c-l, l-c], \\ \int_{x-c}^l f(x') dx', & x \in [l-c, l]. \end{cases} \quad (30)$$

Hence, in this case Eq. (22) yields

$$f(x) = \frac{a}{2c} + \frac{1}{2c} \int_{-l}^{x+c} f(x') dx' \quad (31a)$$

for $x \in [-l, c - l)$,

$$f(x) = \frac{1}{2c} \int_{x-c}^{x+c} f(x') dx' \quad (31b)$$

for $x \in (c - l, l - c)$, and

$$f(x) = \frac{a}{2c} + \frac{1}{2c} \int_{x-c}^l f(x') dx' \quad (31c)$$

75 for $x \in (l - c, l]$.

A remarkable advantage of Eqs. (26), (29) and (31) is that they can be solved analytically and, what is especially important, the choice of $q(z)$ in the form (24) permits us to characterize the complexity of the function $f(x)$ by a single ratio parameter $\sigma = 2l/c$. In particular, it will be demonstrated 80 that, if $\sigma \in (n - 1, n)$ with $n = \overline{1, \infty}$, then $f(x)$ is a piecewise continuous function, which, in general, consists of $2n - 1$ branches. These branches are separated from each other by $2(n - 1)$ points $\pm x_k$, where $k = \overline{1, n - 1}$ ($n \geq 2$) and $x_k = |2k/\sigma - 1|l$, at which the function $f(x)$ can be either continuous or discontinuous (with jump discontinuity). The change of the number of 85 branches occurs at the critical values $\sigma_{\text{cr}} = n - 1$ of the ratio parameter σ . Next, we determine the function $f(x)$ for $n = 1, 2, 3$ and $n \rightarrow \infty$, calculate the probability a , and compare analytical results with those obtained by numerical simulations of Eq. (4).

4.2. Solution at $\sigma \in (0, 1)$

The condition $n = 1$ [i.e., $\sigma \in (0, 1)$] means that $c > 2l$ and hence the function $f(x)$ obeys Eq. (26), according to which $f(x) = f = \text{const}$. The substitution of $f(x) = f$ into Eq. (26) and condition (23) yields a set of equations $f = a/c + fl/c$ and $a = 1/2 - fl$. Solving it with respect to f and a and introducing the reduced non-normalized probability density $\tilde{f}(\tilde{x})$ as $\tilde{f}(\tilde{x}) = f(l\tilde{x})l$ ($\tilde{x} = x/l$) and \tilde{f} as $\tilde{f} = fl$, we obtain

$$\tilde{f} = \frac{\sigma}{4}, \quad a = \frac{1}{2} - \frac{\sigma}{4}. \quad (32)$$

From this, using a general representation

$$\tilde{P}_{\text{st}}(\tilde{x}) = a[\delta(\tilde{x} - 1) + \delta(\tilde{x} + 1)] + \tilde{f}(\tilde{x}) \quad (33)$$

of the reduced PDF $\tilde{P}_{\text{st}}(\tilde{x}) = P_{\text{st}}(l\tilde{x})l$, one gets

$$\tilde{P}_{\text{st}}(\tilde{x}) = \left(\frac{1}{2} - \frac{\sigma}{4}\right) [\delta(\tilde{x} - 1) + \delta(\tilde{x} + 1)] + \frac{\sigma}{4}. \quad (34)$$

90 Thus, at $n = 1$ the non-normalized probability density is uniform, i.e., $\tilde{f}(\tilde{x}) = \tilde{f}$ for all $|\tilde{x}| \leq 1$ (the only one branch exists in this case). According to (32), the probability density \tilde{f} decreases and the probability a increases as the ratio parameter σ decreases. For small σ , these results can be understood by noting that the mean value of $|z_i|$, which we denote as Z , is inversely proportional to σ . Indeed, since $Z = \int_{-\infty}^{\infty} |z|q(z) dz = l/\sigma$, the higher is Z (i.e., the lower is σ), the higher is the probability a and hence the lower is the probability density \tilde{f} . As illustrated in Fig. 1, the above theoretical results are in complete agreement with those obtained by solving Eq. (4) numerically.

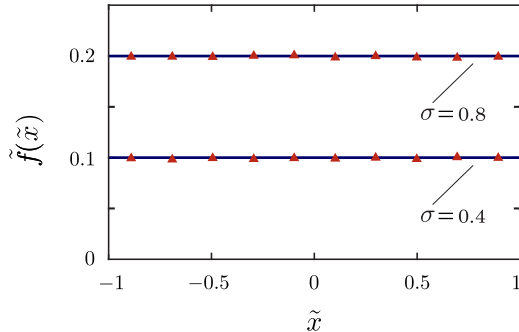


Figure 1: Reduced non-normalized probability density $\tilde{f}(\tilde{x})$ as a function of the reduced variable $\tilde{x} = x/l$ for $\sigma = 0.4$ and $\sigma = 0.8$. The solid horizontal lines represent the theoretical result (32) for \tilde{f} , and triangle symbols represent the results of numerical simulations of Eq. (4). The theoretical values of the probability a ($a = 0.4$ for $\sigma = 0.4$ and $a = 0.3$ for $\sigma = 0.8$) are also in good agreement with the numerical ones ($a \approx a_- \approx a_+$).

100 In order to derive these and other numerical results, we proceed as follows (see also Ref. [31]). First, considering τ as the time step and assuming that $\tau = 10^{-3}$, $l = 1$, $\lambda = 1$ and $X_0 = 0$ (here, the model parameters are chosen to be dimensionless), from Eq. (4) we find $X_{M\tau}$ for $N = 10^6$ simulation runs. Because we are concerned with the stationary state, the number of steps is taken to be large enough: $M = 10^4$. Then, the interval $(-1, 1)$ is divided into $K = 50$ subintervals of width $\delta = 2/K$, and the reduced non-normalized probability density is defined as $\tilde{f}(\bar{x}_m) = N_m/\delta N$, where \bar{x}_m is the middle

110 position of the m -th subinterval, $m = \overline{1, K}$, and N_m is the number of runs for which $X_{M\tau}$ belongs to the m -th subinterval. Finally, the probability a is defined as $a = (a_- + a_+)/2$, where $a_- = N_-/N$, $a_+ = N_+/N$, and N_- and N_+ are the number of runs for which $X_{M\tau} = -l$ and $X_{M\tau} = l$, respectively.

4.3. Solution at $\sigma \in (1, 2)$

If $n = 2$, then $\sigma \in (1, 2)$ and so $c \in (l, 2l)$. Therefore, in this case the non-normalized probability density $f(x)$ must satisfy Eqs. (29). Assuming that $x \in [-l, l - c)$ and taking into account that $\int_{-l}^0 f(x') dx' = (1 - 2a)/2$, we can rewrite Eq. (29a) in the form

$$f(y) = \frac{1}{4c} + \frac{1}{2c} \int_0^{c-l} f(x') dx' + \frac{1}{2c} \int_{c-l}^{y+c} f(x') dx'. \quad (35)$$

Here, for convenience of future calculations, we temporarily replaced the variable x by y . By differentiating Eq. (35) with respect to y , we get the equation

$$\frac{d}{dy} f(y) = \frac{1}{2c} f(y + c), \quad (36)$$

which belongs to a class of differential difference equations (see, e.g., Ref. [33]).

If $x \in (l - c, c - l)$, then, using (29b) and condition (23), we immediately find

$$f(x) = \frac{1}{2c}. \quad (37)$$

With this result, Eq. (35) is reduced to

$$f(y) = \frac{1}{2c} - \frac{l}{4c^2} + \frac{1}{2c} \int_{c-l}^{y+c} f(x') dx'. \quad (38)$$

Finally, if $x \in (c - l, l]$, then it is reasonable to divide the interval of integration in Eq. (29c) by three subintervals $(x - c, l - c)$, $(l - c, 0)$ and $(0, l]$. This, together with the above results (23), (37) and condition $x = y + c$, permits us to represent Eq. (29c) in the form

$$f(y + c) = \frac{1}{2c} - \frac{l}{4c^2} + \frac{1}{2c} \int_y^{l-c} f(x') dx', \quad (39)$$

which, after differentiating with respect to y , yields the following differential difference equation:

$$\frac{d}{dy}f(y+c) = -\frac{1}{2c}f(y). \quad (40)$$

A set of differential difference equations (36) and (40) determines the non-normalized probability density on the intervals $[-l, l-c]$ and $(c-l, l]$. Its remarkable feature is that it can be reduced (by a single differentiation of these equations with respect to y) to a set of independent ordinary differential equations

$$\frac{d^2}{dy^2}f(y) + \frac{1}{4c^2}f(y) = 0, \quad (41a)$$

$$\frac{d^2}{dy^2}f(y+c) + \frac{1}{4c^2}f(y+c) = 0. \quad (41b)$$

Since $-y \in (c-l, l]$ and $f(-y) = f(y)$, Eq. (41b) is equivalent to Eq. (41a). Therefore, returning to the variable x , from the equation

$$\frac{d^2}{dx^2}f(x) + \frac{1}{4c^2}f(x) = 0 \quad (42)$$

we find the function $f(x)$ at $x \in [-l, l-c]$,

$$f(x) = \alpha \cos \frac{x}{2c} + \beta \sin \frac{x}{2c} \quad (43)$$

(α and β are parameters to be determined), and at $x \in (c-l, l]$,

$$f(x) = \alpha' \cos \frac{x}{2c} + \beta' \sin \frac{x}{2c}. \quad (44)$$

Taking also into account that $f(-x) = f(x)$, one can make sure that $\alpha' = \alpha$ and $\beta' = -\beta$. Thus, collecting the above results, for the non-normalized probability density $f(x)$ we obtain a general representation

$$f(x) = \begin{cases} \alpha \cos(x/2c) + \beta \sin(x/2c), & x \in [-l, l-c], \\ 1/2c, & x \in (l-c, c-l), \\ \alpha \cos(x/2c) - \beta \sin(x/2c), & x \in (c-l, l]. \end{cases} \quad (45)$$

To find the parameters α and β , we use Eq. (38) with $y = x \in [-l, l-c]$. Substituting (45) into Eq. (38), we arrive to the equation

$$\begin{aligned} & \left[\alpha \left(1 - \sin \frac{1}{2} \right) - \beta \cos \frac{1}{2} \right] \cos \frac{x}{2c} + \left[\beta \left(1 + \sin \frac{1}{2} \right) - \alpha \cos \frac{1}{2} \right] \sin \frac{x}{2c} \\ & + \alpha \sin \frac{c-l}{2c} + \beta \cos \frac{c-l}{2c} - \frac{1}{2c} + \frac{l}{4c^2} = 0. \end{aligned} \quad (46)$$

It holds for all x only if three conditions

$$\alpha \left(1 - \sin \frac{1}{2}\right) - \beta \cos \frac{1}{2} = 0, \quad \beta \left(1 + \sin \frac{1}{2}\right) - \alpha \cos \frac{1}{2} = 0, \quad (47a)$$

$$\alpha \sin \frac{c-l}{2c} + \beta \cos \frac{c-l}{2c} - \frac{1}{2c} + \frac{l}{4c^2} = 0 \quad (47b)$$

are simultaneously satisfied. Since conditions in (47a) are equivalent (this can be verified directly), we can consider one of them (e.g., the first one) and condition (47b) as a set of linear equations for α and β . The straightforward solution of these equations leads to

$$\alpha = \frac{1}{l} \frac{\sigma(1 - \sigma/4) \cos [(\pi - 1)/4]}{4 \cos [(\sigma + \pi - 1)/4]}, \quad \beta = \frac{1}{l} \frac{\sigma(1 - \sigma/4) \sin [(\pi - 1)/4]}{4 \cos [(\sigma + \pi - 1)/4]}. \quad (48)$$

Formulas (45) and (48) completely determine the non-normalized probability density function $f(x)$ in the case when $\sigma \in (1, 2)$. Since $f(x)$ is expressed in terms of trigonometric functions, integral in (45) can be calculated analytically, yielding

$$a = \frac{\sigma}{4} - \sqrt{2} \frac{(1 - \sigma/4) \sin [(\sigma - 1)/4]}{\cos [(\sigma + \pi - 1)/4]}. \quad (49)$$

For convenience of analysis, we rewrite the non-normalized probability density (45) in the reduced form

$$\tilde{f}(\tilde{x}) = \begin{cases} \alpha l \cos(\sigma \tilde{x}/4) + \beta l \sin(\sigma \tilde{x}/4), & x \in [-1, -\tilde{x}_1), \\ \sigma/4, & x \in (-\tilde{x}_1, \tilde{x}_1), \\ \alpha l \cos(\sigma \tilde{x}/4) - \beta l \sin(\sigma \tilde{x}/4), & x \in (\tilde{x}_1, 1], \end{cases} \quad (50)$$

where $\tilde{x}_1 = |2/\sigma - 1|$ (this definition of \tilde{x}_1 will be used for $\sigma \in (2, 3)$ as well). The properties of this probability density are surprising and unexpected. Indeed, in contrast to the previous case, in this case the function $\tilde{f}(\tilde{x})$ has three branches and it is discontinuous at $\tilde{x} = \pm\tilde{x}_1$. We emphasize that this qualitative change of the behavior of $\tilde{f}(\tilde{x})$ occurs when the ratio parameter σ exceeds the critical one $\sigma_{\text{cr}} = 1$. Using (50) and (48), it can be shown that

$$\tilde{f}(\pm 1) = \frac{\sigma}{4} \left(1 - \frac{\sigma}{4}\right), \quad \tilde{f}(\pm\tilde{x}_1 \pm 0) = \frac{\sigma}{4} \left(1 - \frac{\sigma}{4}\right) \tan \frac{\sigma + \pi - 1}{4} \quad (51)$$

115 and $\tilde{f}(\pm 1) < \tilde{f}(\pm\tilde{x}_1 \pm 0) < \sigma/4$. With increasing σ from 1 to 2, the width of the intervals $[-1, -\tilde{x}_1)$ and $(\tilde{x}_1, 1]$, where $\tilde{f}(\tilde{x})$ nonlinearly depends on \tilde{x} ,

increases from 0 to 1, and the width of the interval $(-\tilde{x}_1, \tilde{x}_1)$, where $\tilde{f}(\tilde{x})$ does not depend on \tilde{x} , decreases from 2 to 0.

For the sake of illustration, in Fig. 2 we show the behavior of the reduced non-normalized probability density (50) for two values of the ratio parameter σ (solid lines). In order to verify these theoretical results, we performed numerical simulations of Eq. (4), paying a special attention to the vicinities of the points of discontinuity $\pm\tilde{x}_1$. As seen from this figure, the numerical results (denoted by triangle symbols) are fully consistent with the theoretical ones.

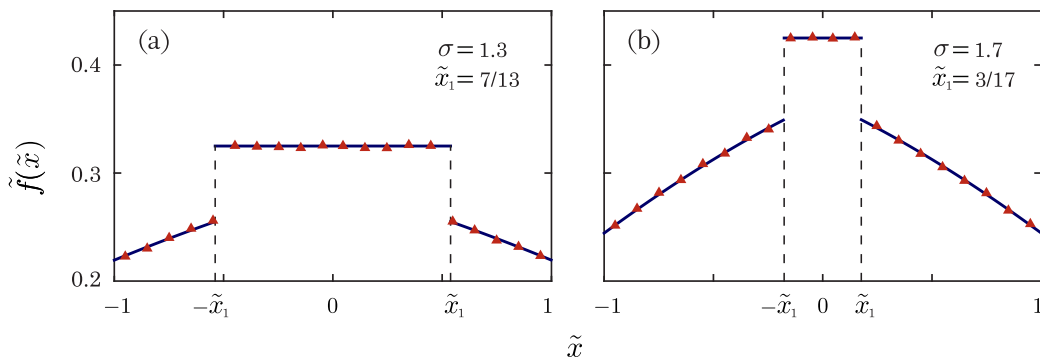


Figure 2: Reduced non-normalized probability density $\tilde{f}(\tilde{x})$ as a function of the reduced variable $\tilde{x} = x/l$ for $\sigma = 1.3$ (a) and $\sigma = 1.7$ (b). The solid lines show theoretical dependencies obtained from (50) and (48), and the triangle symbols indicate the results obtained by numerical simulations of Eq. (4).

125

4.4. Solution at $\sigma \in (2, 3)$

To determine the non-normalized probability density $f(x)$ at $n = 3$, i.e., when $\sigma \in (2, 3)$ or, equivalently, when $c \in (2l/3, l)$, we should use Eqs. (31). Since in this case the chain of inequalities $-l < l - 2c < c - l < l - c < 2c - l < l$ holds, it is reasonable to divide the interval $[-l, l]$ into five subintervals $[-l, l - 2c)$, $(l - 2c, c - l)$, $(c - l, l - c)$, $(l - c, 2c - l)$ and $(2c - l, l]$. Then, using formula (23), from Eq. (31a) one can derive the equations

$$f(y_1) = \frac{1}{4c} + \frac{1}{2c} \int_0^{y_1+c} f(x') dx' \quad (52)$$

and

$$\frac{d}{dy_1} f(y_1) = \frac{1}{2c} f(y_1 + c), \quad (53)$$

if $y_1 \in [-l, l - 2c)$, and the equations

$$f(y_2) = \frac{1}{4c} + \frac{1}{2c} \int_0^{l-c} f(x') dx' + \frac{1}{2c} \int_{l-c}^{y_2+c} f(x') dx' \quad (54)$$

and

$$\frac{d}{dy_2} f(y_2) = \frac{1}{2c} f(y_2 + c), \quad (55)$$

if $y_2 \in (l - 2c, c - l)$ (we temporary use the variables y_1 and y_2 instead of the variable x).

Similarly, Eq. (31b) at $x = y_1 + c \in (c - l, l - c)$ yields the equation

$$f(y_1 + c) = \frac{1}{2c}(1 - 2a) - \frac{1}{2c} \int_{-l}^{y_1} f(x') dx' - \frac{1}{2c} \int_{y_1+2c}^l f(x') dx', \quad (56)$$

from which one immediately obtains

$$\frac{d}{dy_1} f(y_1 + c) = -\frac{1}{2c} f(y_1) + \frac{1}{2c} f(y_1 + 2c). \quad (57)$$

Finally, from Eq. (31c) we find the equations

$$f(y_2 + c) = \frac{1}{4c} + \frac{1}{2c} \int_{c-l}^0 f(x') dx' + \frac{1}{2c} \int_{y_2}^{c-l} f(x') dx' \quad (58)$$

and

$$\frac{d}{dy_2} f(y_2 + c) = -\frac{1}{2c} f(y_2), \quad (59)$$

if $x = y_2 + c \in (l - c, 2c - l)$, and the equations

$$f(y_1 + 2c) = \frac{1}{4c} + \frac{1}{2c} \int_{y_1+c}^0 f(x') dx' \quad (60)$$

and

$$\frac{d}{dy_1} f(y_1 + 2c) = -\frac{1}{2c} f(y_1 + c), \quad (61)$$

if $x = y_1 + 2c \in (2c - l, l]$.

Let us first consider two sets of the above differential difference equations, namely, a set of Eqs. (53), (57) and (61), and a set of Eqs. (55) and (59). Remarkably, each of these sets can also be reduced to a set of independent

ordinary differential equations that are easily solved. In particular, by differentiating Eq. (57) with respect to y_1 and using Eqs. (53) and (61), we get

$$\frac{d^2}{dy_1^2}f(y_1 + c) + \frac{1}{2c^2}f(y_1 + c) = 0. \quad (62)$$

Returning to the variable $x = y_1 + c$, the symmetric solution of this equation can be represented as

$$f(x) = \mu \cos \frac{x}{\sqrt{2c}}, \quad (63)$$

where $x \in (c - l, l - c)$ and μ is a parameter to be determined. Then, substituting $f(y_1 + c)$ from Eq. (53) into Eq. (62) and returning to the variable x , one obtains the equation

$$\frac{d^3}{dx^3}f(x) + \frac{1}{2c^2} \frac{d}{dx}f(x) = 0, \quad (64)$$

which holds for both $x \in [-l, l - 2c]$ and $x \in (2c - l, l]$. Using the symmetry condition $f(-x) = f(x)$, the solution of this equation can be written in the form

$$f(x) = \begin{cases} \eta \cos(x/\sqrt{2c}) + \kappa \sin(x/\sqrt{2c}) + \gamma, & x \in [-l, l - 2c], \\ \eta \cos(x/\sqrt{2c}) - \kappa \sin(x/\sqrt{2c}) + \gamma, & x \in (2c - l, l]. \end{cases} \quad (65)$$

Similarly, it can be shown that the set of Eqs. (55) and (59) is reduced to Eq. (42), which holds on intervals $(l - 2c, c - l)$ and $(l - c, 2c - l)$. The solution of this equation, satisfying the condition $f(-x) = f(x)$, is given by

$$f(x) = \begin{cases} \nu \cos(x/2c) + \chi \sin(x/2c), & x \in (l - 2c, c - l), \\ \nu \cos(x/2c) - \chi \sin(x/2c), & x \in (l - c, 2c - l). \end{cases} \quad (66)$$

To determine the unknown parameters in (63), (65) and (66), we use Eqs. (52), (54) and (56). Substituting $f(x)$ from (63), (65) and (66) into these equations and omitting technical details, we obtain the following representation for the non-normalized probability density:

$$f(x) = \begin{cases} (\mu/\sqrt{2}) \sin[(c+x)/\sqrt{2c}] + 1/4c, & x \in [-l, l - 2c], \\ \nu (\cos(x/2c) + \sin[(c+x)/2c]), & x \in (l - 2c, c - l), \\ \mu \cos(x/\sqrt{2c}), & x \in (c - l, l - c), \\ \nu (\cos(x/2c) + \sin[(c-x)/2c]), & x \in (l - c, 2c - l), \\ (\mu/\sqrt{2}) \sin[(c-x)/\sqrt{2c}] + 1/4c, & x \in (2c - l, l], \end{cases} \quad (67)$$

where

$$\mu = \frac{\sigma}{8l} \frac{1}{\sin[(\sigma/2 - 1)/\sqrt{2}]} \frac{\sigma/2 - 3 + 2 \cot[(\sigma + \pi - 3)/4]}{\cot[(\sigma/2 - 1)/\sqrt{2}] - \sqrt{2} \cot[(\sigma + \pi - 3)/4]} \quad (68)$$

and

$$\nu = \frac{\sigma}{16l} \frac{\cos(1/4) - \sin(1/4)}{\cos(1/2) \sin[(\sigma + \pi - 3)/4]} \frac{\sigma/2 - 3 + \sqrt{2} \cot[(\sigma/2 - 1)/\sqrt{2}]}{\cot[(\sigma/2 - 1)/\sqrt{2}] - \sqrt{2} \cot[(\sigma + \pi - 3)/4]}. \quad (69)$$

Finally, by direct integration of $f(x)$, from (23) one gets

$$a = \frac{3}{2} - \frac{\sigma}{4} - \frac{\sqrt{2}}{4} \frac{\sigma/2 - 3 + \sqrt{2} \cot[(\sigma/2 - 1)/\sqrt{2}]}{\cot[(\sigma/2 - 1)/\sqrt{2}] - \sqrt{2} \cot[(\sigma + \pi - 3)/4]} \cot \frac{\sigma + \pi - 3}{4}. \quad (70)$$

In the reduced form, the non-normalized probability density (67) is rewritten as

$$\tilde{f}(\tilde{x}) = \begin{cases} (\mu l/\sqrt{2}) \sin[(c+x)/\sqrt{2}c] + \sigma/8, & x \in [-1, -\tilde{x}_2), \\ \nu l (\cos(x/2c) + \sin[(c+x)/2c]), & x \in (-\tilde{x}_2, -\tilde{x}_1), \\ \mu l \cos(x/\sqrt{2}c), & x \in (-\tilde{x}_1, \tilde{x}_1), \\ \nu l (\cos(x/2c) + \sin[(c-x)/2c]), & x \in (\tilde{x}_1, \tilde{x}_2), \\ (\mu l/\sqrt{2}) \sin[(c-x)/\sqrt{2}c] + \sigma/8, & x \in (\tilde{x}_2, 1], \end{cases} \quad (71)$$

130 where $\tilde{x}_2 = |4/\sigma - 1|$ and $\tilde{x}_1 < \tilde{x}_2 < 1$. In accordance with the general
rule formulated at the end of Section 4.1, in this case the function $\tilde{f}(\tilde{x})$
has five branches separated from each other by four points $\pm\tilde{x}_1$ ($\tilde{f}(\tilde{x})$ is
discontinuous at $\tilde{x} = \pm\tilde{x}_1$) and $\pm\tilde{x}_2$ ($\tilde{f}(\tilde{x})$ is continuous at $\tilde{x} = \pm\tilde{x}_2$). The
intervals $[-1, -\tilde{x}_2)$, $(-\tilde{x}_1, \tilde{x}_1)$ and $(\tilde{x}_2, 1]$ have the same width $2 - 4/\sigma$, which
135 increases from 0 to $2/3$ as the ratio parameter σ grows from 2 to 3. In
contrast, the width $6/\sigma - 2$ of the intervals $(-\tilde{x}_2, -\tilde{x}_1)$ and $(\tilde{x}_1, \tilde{x}_2)$ decreases
from 1 to 0. As in the previous cases, the theoretical results obtained for
 $\sigma \in (2, 3)$ are confirmed by numerical simulations, see Fig. 3.

4.5. Solution at $\sigma \rightarrow \infty$

The above results indicate that, because the number of branches of the non-normalized PDF $f(x)$ grows, its local behavior becomes more and more complex with increasing parameter σ (we recall, σ is the ratio of the domain size $2l$ of the bounded process X_t to the half-width c of uniform distribution

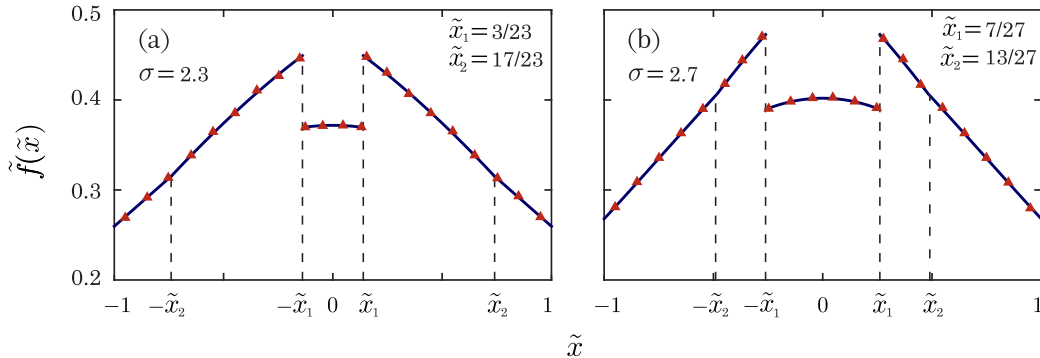


Figure 3: Reduced non-normalized probability density $\tilde{f}(\tilde{x})$ as a function of the reduced variable $\tilde{x} = x/l$ for $\sigma = 2.3$ (a) and $\sigma = 2.7$ (b). The solid lines represent the theoretical results obtained using (71), (68) and (69), and the triangle symbols show the numerical results obtained by numerical simulations of Eq. (4).

of jump magnitudes z_i). For this reason, we were not able to solve Eqs. (31) analytically for arbitrary large values of σ (we solved it for $n = 4$ as well, but the results are too cumbersome to present here). However, the function $f(x)$ in the limit $\sigma \rightarrow \infty$ approaches a constant, which can be determined as follows. First, using (27), we find

$$\int_{-l}^l q(x - x') dx' = \frac{1}{2c} \times \begin{cases} l + c + x, & x \in [-l, c - l], \\ 2c, & x \in [c - l, l - c], \\ l + c - x, & x \in [l - c, l]. \end{cases} \quad (72)$$

Then, assuming that $f(x) = h = \text{const}$ and substituting expressions (27) and (72) into Eq. (22), one can make sure that at $x \in (-l + c, l - c)$ this equation is satisfied identically, and at $x \in [-l, -l + c]$ it reduces to

$$h = \frac{a}{2c} + h \frac{l + c + x}{2c}. \quad (73)$$

140 (Note, at $x \in [l - c, l]$ Eq. (22) reduces to Eq. (73) with x replaced by $-x$.)

As it follows from Eq. (73), our assumption that $f(x)$ does not depend on x is, strictly speaking, incorrect. Nevertheless, if $c \ll l$ (i.e., $\sigma \gg 1$), it can be used as a first approximation. Indeed, taking into account that, according to (23), $a = 1/2 - hl$, from Eq. (73) one obtains

$$h = \frac{1}{2l} \frac{1}{1 + (c - l - x)/l}. \quad (74)$$

Since the values of $c - l - x$ for $x \in [-l, -l + c]$ belong to the interval $[0, c]$ and the condition $c \ll l$ holds, we get $h = 1/2l$ and $a = 0$ as $\sigma \rightarrow \infty$. Hence, in this limit the reduced PDF (33) takes the form

$$\tilde{P}_{\text{st}}(\tilde{x})|_{\sigma \rightarrow \infty} = \frac{1}{2} \quad (|\tilde{x}| \leq 1). \quad (75)$$

Our numerical simulations show that (if $\sigma \gtrsim 50$) this result is reproduced with an accuracy of a few percent or better [to estimate the accuracy analytically, one can use formula (77)]. It should be noted in this regard that with increasing σ the number of time steps M , which is necessary to reach the stationary state, increases as well. We also stress that the same result (75) holds for the bounded process X_t driven by Gaussian white noise [4].

4.6. Extreme values probability

The probability a that in the stationary state $X_t = -l$ (or $X_t = l$) is determined by the formulas (32), (49) and (70) for $\sigma \in (0, 1)$, $\sigma \in (1, 2)$ and $\sigma \in (2, 3)$, respectively. Using these formulas, it can be directly shown that $a|_{\sigma=1-0} = a|_{\sigma=1+0}$ and $a|_{\sigma=2-0} = a|_{\sigma=2+0}$, i.e., a is a continuous function of σ at the critical points $\sigma_{\text{cr}} = 1$ and $\sigma_{\text{cr}} = 2$, and a monotonically decreases as the ratio parameter σ increases from 0 to 3. As Fig. 4 illustrates, our theoretical results (32), (49) and (70) are in excellent agreement with the simulation data.

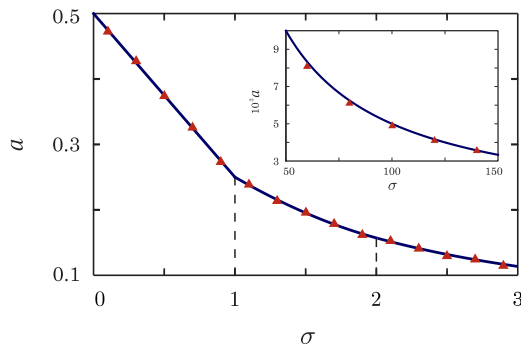


Figure 4: Probability a of the extremal values of the bounded process X_t as a function of the ratio parameter σ . The solid lines represent the theoretical results (32), (49) and (70) for $\sigma \in (0, 1)$, $\sigma \in (1, 2)$ and $\sigma \in (2, 3)$, respectively. The results obtained via numerical simulations of Eq. (4) are marked by triangle symbols. Inset: probability a vs. σ for large values of σ . The solid line represents the asymptotic formula $a = 1/2\sigma$.

Although we have no explicit expressions for the probability a at $\sigma > 3$, it can be easily seen that a as a function of σ is continuous at the critical points $\sigma_{\text{cr}} = \overline{3, \infty}$ as well. Indeed, according to the properties of $f(x)$ formulated in [Section 4.1](#), the function $f(x)$ at $\sigma = \sigma_{\text{cr}}+0$ acquires new branches (compared to $\sigma = \sigma_{\text{cr}} - 0$), which are located at separate points. Since these points do not contribute to the integral in [\(23\)](#), one may conclude that $a|_{\sigma=\sigma_{\text{cr}}-0} = a|_{\sigma=\sigma_{\text{cr}}+0}$, i.e., the probability a as a function of the ratio parameter σ is continuous at all critical points $\sigma = \sigma_{\text{cr}}$.

Using results of the previous section, we can also estimate the dependence of a on σ for $\sigma \gg 1$. To this end, we first note that, according to our assumption $f(x) = h = \text{const}$, the condition $\int_{-l}^l f(x) dx = 2lh$ must hold. On the other hand, from the above results it follows that

$$\int_{-l}^l f(x) dx = 2(l-c)h + \frac{1}{2} \int_{-l}^{-l+c} \frac{dx}{c-x} + \frac{1}{2} \int_{l-c}^l \frac{dx}{c+x}. \quad (76)$$

Performing integration and equating the right-hand side of [\(76\)](#) to $2lh$, we obtain

$$h = \frac{\sigma}{4l} \ln \left(1 + \frac{2}{\sigma} \right) \quad (77)$$

and, since $a = 1/2 - lh$,

$$a = \frac{1}{2} - \frac{\sigma}{4} \ln \left(1 + \frac{2}{\sigma} \right). \quad (78)$$

Taking into account that the ratio parameter σ is assumed to be large enough, from [\(78\)](#) one gets in the first nonvanishing approximation: $a = 1/2\sigma$ as $\sigma \rightarrow \infty$. Our numerical results confirm this theoretical prediction, see inset in [Fig. 4](#) (note, to reach the stationary state at $\sigma \in (50, 150)$, the number of steps M was chosen to be $3 \cdot 10^8$).

5. Conclusions

We have studied the statistical properties of a class of bounded jump processes governed by a special case of the difference Langevin equation driven by Poisson white noise, i.e., a random sequence of delta pulses. In contrast to the ordinary Langevin equation, this equation, due to the use of the saturation function, has only bounded solutions. We have derived the Kolmogorov-Feller equation for the normalized probability density function

(PDF) of these processes and found its stationary solutions in the case of the uniform distribution of pulse sizes, which is assumed to be symmetric. It has been explicitly shown that the stationary PDF can be decomposed into two singular terms defining the probability of the process extreme values and a regular part representing the non-normalized PDF inside a bounded domain. Amazingly, the non-normalized PDF has proven to be a complex piecewise function with jump discontinuities.

One of the most remarkable findings is that the ratio of the width of the saturation function to the half-width of the uniform distribution of pulse sizes is the only parameter which controls all properties of the stationary PDF. In particular, the ratio parameter determines the number of branches of the non-normalized PDF and coordinates of points separating these branches. It has been also established that, with its increasing, two new branches are created every time the ratio parameter is equal to a natural number. Interestingly, although this enhances the local complexity of the stationary PDF, it approaches a constant in the limit of large values of the ratio parameter. All our theoretical predictions have been confirmed by numerical simulations of the difference Langevin equation.

To the best of our knowledge, the proposed Langevin model of bounded jump processes driven by Poisson white noise is the first one that allows to study the nontrivial statistical properties of these processes in great analytical detail.

Acknowledgment

This work was partially supported by the Ministry of Education and Science of Ukraine under Grant No. 0119U100772.

References

- [1] Coffey WT, Kalmykov YuP, Waldron JT. The Langevin Equation: With Applications in Physics
- [2] Risken R. The Fokker-Planck Equation. Second edition, third printing. Berlin: Springer-Verlag
- [3] Horsthemke W, Lefever R. Noise-Induced Transitions. Theory and Applications in Physics, C
- [4] Gardiner CW. Stochastic Methods: A Handbook for the Natural and Social sciences. Fourth
- [5] Sancho JM, San Miguel M. Langevin equations with colored noise. In: Moss F, McClintock R

- [6] Lindenberg K, West BJ. The Nonequilibrium Statistical Mechanics of Open and Closed Systems. Springer, 2008.
- [7] Hänggi P, Jung P. Colored noise in dynamical systems. In: Prigogine I, Rice SA, editors. Adv Chem Phys. Wiley, 1995; 102:1-135.
- [8] Wang P, Tartakovsky AM, Tartakovsky DM. Probability density function method for Langevin equations. J Comput Phys. 2004; 197:1-15.
- 210 [9] Maltba T, Gremaud PA, Tartakovsky DM. Nonlocal PDF methods for Langevin equations with multiplicative noise. J Comput Phys. 2008; 223:1-15.
- [10] Denisov SI, Horsthemke W. Statistical properties of a class of nonlinear systems driven by colored noise. Phys Rev E. 2004; 70:016101.
- [11] Denisov SI, Horsthemke W. Exactly solvable model with an absorbing state and multiplicative noise. Phys Rev E. 2005; 72:016101.
- [12] Vitrenko AN. Exactly solvable nonlinear model with two multiplicative Gaussian colored noises. Phys Rev E. 2006; 74:016101.
- [13] Hänggi P. Langevin description of Markovian integro-differential master equations. Z Phys B. 1984; 61:1-10.
- 215 [14] Hernández-García E, Pesquera L, Rodríguez MA, San Miguel M. First-passage time statistics of a stochastic system with a reflecting boundary. Phys Rev E. 2005; 72:016101.
- [15] Luczka J, Bartussek R, Hänggi P. White-noise-induced transport in periodic structures. Euro Phys J B. 2000; 13:1-10.
- [16] Grigoriu M. Stochastic Calculus: Applications in Science and Engineering. Boston: Birkhäuser, 2005.
- [17] Gitterman M. The Noisy Oscillator. Singapore: World Scientific; 2005.
- [18] Baule A, Sollich P. Rectification of asymmetric surface vibrations with dry friction: An exact solution. Phys Rev E. 2004; 70:016101.
- 220 [19] Spiechowicz J, Hänggi P, Luczka J. Brownian motors in the microscale domain: Enhancement of transport by noise. Phys Rev E. 2005; 72:016101.
- [20] He M, Xu W, Sun Z, Jia W. Characterizing stochastic resonance in coupled bistable system with Poisson white noise. Phys Rev E. 2006; 74:016101.
- [21] Zhu HT. Stochastic response of a vibro-impact Duffing system under external Poisson impulses. Phys Rev E. 2007; 75:016101.
- [22] Yang G, Xu W, Huang D, Hao M. Stochastic responses of lightly nonlinear vibroimpact systems. Phys Rev E. 2008; 78:016101.
- [23] Pan SS, Zhu WQ. Dynamics of a prey-predator system under Poisson white noise excitation. Phys Rev E. 2009; 80:016101.
- 225 [24] Jia W, Xu Y, Li D. Stochastic dynamics of a time-delayed ecosystem driven by Poisson white noise. Phys Rev E. 2010; 82:016101.
- [25] Vasta M. Exact stationary solution for a class of non-linear systems driven by a non-normal colored noise. Phys Rev E. 2004; 70:016101.
- [26] Proppe C. Exact stationary probability density functions for non-linear systems under Poisson white noise. Phys Rev E. 2005; 72:016101.
- [27] Denisov SI, Horsthemke W, Hänggi P. Generalized Fokker-Planck equation: Derivation and exact solution. Phys Rev E. 2006; 74:016101.
- [28] Rudenko OV, Dubkov AA, Gurbatov SN. On exact solutions to the Kolmogorov-Feller equation. Phys Rev E. 2007; 75:016101.

- 230 [29] Dubkov AA, Rudenko OV, Gurbatov SN. Probability characteristics of nonlinear dynamical s
- [30] d'Onofrio A, editor. Bounded Noises in Physics, Biology, and Engineering. New York: Birkh
- [31] Denisov SI, Bystrik Yu.S. Statistics of bounded processes driven by Poisson white noise. Phys
- [32] Denisov SI, Vitrenko AN, Horsthemke W. Nonequilibrium transitions induced by the cross-co
- [33] Bellman R, Cooke KL. Differential-Difference Equations. New York: Academic Press; 1963.